

Antiferromagnetic Ising Model on Inverse Perovskite Lattice

Daisuke TAHARA, Yukitoshi MOTOME¹ and Masatoshi IMADA¹

Department of Physics, University of Tokyo, 7-3-1 Hongo, Bunkyo-ku, Tokyo 113-0033

¹*Department of Applied Physics, University of Tokyo, 7-3-1 Hongo, Bunkyo-ku, Tokyo 113-8656*

We study thermodynamic properties of an antiferromagnetic Ising model on the inverse perovskite lattice by using Monte Carlo simulations. The lattice structure is composed of corner-sharing octahedra and contains three-dimensional geometrical frustration in terms of magnetic interactions. The system with the nearest-neighbor interactions alone does not exhibit any phase transition, leading to a degenerate ground state with large residual entropy. The degeneracy is lifted by an external magnetic field or by an anisotropy in the interactions. Depending on the anisotropy, they stabilize either a 3D ferrimagnetic state or a partially-disordered antiferromagnetic (PDAF) state with a dimensionality reduction to 2D. By the degeneracy-lifting perturbations, all the transition temperatures of these different ordered states continuously grow from zero, leaving an unusual zero-temperature critical point at the unperturbed point. Such a zero-temperature multicriticality is not observed in other frustrated structures such as face-centered cubic and pyrochlore. The transition to the PDAF state is represented by either the first- or second-order boundaries separated by tricritical lines, whereas the PDAF phase shows 1/3 magnetization plateaus.

KEYWORDS: geometrical frustration, inverse perovskite, Ising model, residual entropy, magnetization plateau, partial disorder, dimensionality reduction, ferrimagnetism

Geometrical frustration is one of the long-standing issues in condensed matter physics. The problem has been intensively investigated in antiferromagnetic (AF) spin systems. Frustration, in general, suppresses the formation of simple-minded long-range orders (LRO) and opens the possibility of interesting phenomena such as a degenerate ground-state manifold with an extensive residual entropy, complicated ordering structures, and spin-liquid states.¹⁾

Even in one of the simplest models, namely the Ising model, frustration leads to intriguing properties.^{1),2)} A prototypical example is the AF Ising model on a triangular lattice. The system does not show any LRO down to zero temperature, and the ground state has macroscopic degeneracy.³⁾⁻⁵⁾ Among other frustrated lattices, 3D models have also attracted considerable attention partly because certain real materials are available as their experimental counterparts. For instance, the face-centered cubic (fcc) lattice has been studied for the problem of binary alloys and the pyrochlore lattice has

been examined to describe magnetite⁶⁾ and spin-ice compounds.⁷⁾

In this paper, we discuss a new 3D frustrated Ising model, an inverse perovskite AF Ising model. The inverse perovskite lattice consists of a simple cubic lattice of octahedra which share their corners, as shown in Fig. 1(a). The corner-sharing geometry reminds us of the well-studied pyrochlore lattice, which consists of corner-sharing tetrahedra. Alternatively, the lattice structure is viewed as an alternating stack of 2D square lattices with different lattice constants along the [001] direction (or the equivalent [100] or [010] direction), while it is a stack of Kagomé lattices along the [111] direction (or the equivalent directions such as $[1\bar{1}\bar{1}]$). These stacks are similar to another well-studied lattice, the fcc lattice, which is a stacking of 2D square (triangular) lattices along the [001] ($[111]$) direction. The inverse perovskite structure

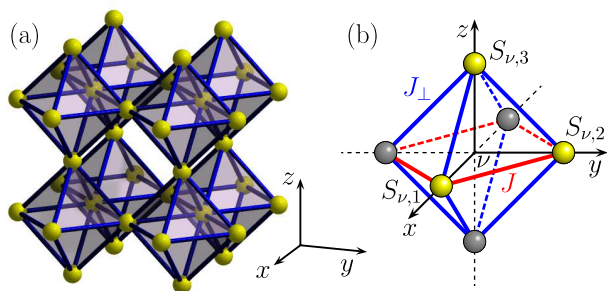


Fig. 1. (a) Inverse perovskite lattice structure. (b) A unit cell with three sublattice sites. J and J_{\perp} are the interactions in the Hamiltonian in eq. (1).

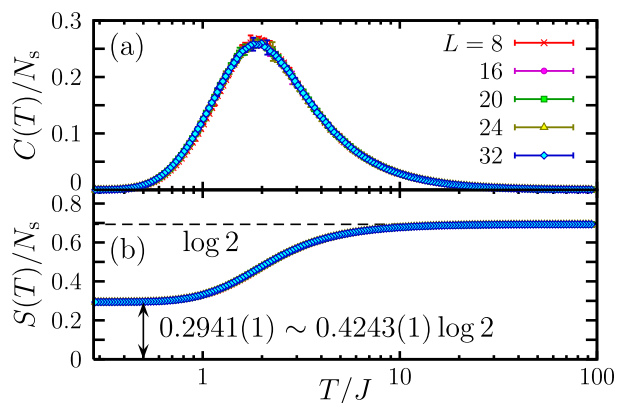


Fig. 2. Temperature dependences of (a) specific heat per site and (b) entropy per site at $J = J_{\perp}$ and $h = 0$. The dashed line in (b) denotes the value in the high-temperature limit, $\log 2$.

is found in several materials such as the superconductor MgCNi₃⁸⁾ and the negative thermal expansion material Mn₃(Cu_{1-x}Ge_x)N.⁹⁾

In the present study, we investigate effects of frustration on the thermodynamics of the AF Ising model on the inverse perovskite lattice. By employing a Monte Carlo (MC) method, we study phase transitions in this model by tuning the degree of frustration and obtain the phase diagram in a wide range of parameters. In addition to some similar behaviors to the fcc and pyrochlore systems, we find a peculiar critical point where all the transition temperatures are suppressed down continuously to zero due to a characteristic structure of the degenerate ground-state manifold in the inverse perovskite system.

Our model Hamiltonian is defined in the form

$$\mathcal{H} = J \sum_{\langle i,j \rangle \in \parallel} S_i S_j + J_{\perp} \sum_{\langle i,j \rangle \in \perp} S_i S_j - h \sum_i S_i, \quad (1)$$

where $S_i = \pm 1$ denotes the Ising variable and h is an external magnetic field. In the inverse perovskite structure, three sites are present in a unit cell, as shown in Fig. 1(b), and S_i in eq. (1) symbolically represents $S_{\nu,\alpha}$, where ν denotes the unit cell and $\alpha = 1, 2$, or 3 is the sublattice index. The summations of the interaction terms are taken over the nearest-neighbor sites on the inverse perovskite lattice in Fig. 1(a), and an anisotropy is introduced in the interactions J and J_{\perp} , as shown in Fig. 1(b): J is for pairs of $S_{\nu,1}$ and $S_{\nu,2}$ spins within the same xy plane, and J_{\perp} is for pairs including $S_{\nu,3}$ spins. We consider both cases of $J > J_{\perp} > 0$ and $J_{\perp} > J > 0$.

We study thermodynamic properties of the model in eq. (1) by using MC simulations. To avoid the critical slowing down in the frustrated system, we employ the exchange MC method¹⁰⁾ by an exchange sampling taken after every 5 standard MC steps. Typically, we perform 10^5 – 10^7 exchanges in total for the system size L^3 ($N_s = 3L^3$ spins) up to $L = 64$ under the periodic boundary conditions. We set the Boltzmann constant $k_B = 1$.

First, we study the isotropic case $J = J_{\perp}$ at the magnetic field $h = 0$. Figure 2(a) shows the temperature (T) dependence of the specific heat per spin plotted in the logarithmic scale of T . The specific heat is calculated by $C(T) = (\langle \mathcal{H}^2 \rangle - \langle \mathcal{H} \rangle^2)/T^2$, where the bracket denotes the thermal average. As shown in Fig. 2(a), the specific heat shows no singularity, except for a broad hump at $T/J \sim 2$ which is almost system-size independent. This indicates that the model does not exhibit any phase transition at finite T . The entropy is calculated by $S(T) = E(T)/T - \int_0^{1/T} E(T') d(1/T') + S(\infty)$, where $E(T) = \langle \mathcal{H} \rangle$ is the internal energy and $S(\infty) = N_s \log 2$ is the entropy in the high- T limit. The result is plotted in Fig. 2(b). With lowering T , the entropy gradually decreases and approaches a finite value as $T \rightarrow 0$. The residual entropy per spin is estimated as $0.2941(1) \sim 42\%$ of $\log 2$ (statistical errors in the last digit are shown in the parentheses, hereafter). This result means that macroscopic degeneracy remains in the ground state. The absence of a phase transition and the large residual entropy are found in other 3D frustrated AF Ising systems such as pyrochlore⁷⁾ and garnet,¹¹⁾ and appears to be a common feature of corner-sharing-type frustrations.

When a magnetic field is applied, the macroscopic degeneracy is lifted and a phase transition takes place at finite T . Figure 3(a) shows T dependences of the specific heat. The specific heat shows a sharp singularity for $|h| > 0$, indicating a phase transition; for instance, a sharp peak at $T/J \sim 1.1$ (2.0) for $h/J = 0.5$ (4.0) as shown in Fig. 3(a). The small hump at $T/J \sim 0.3$ for $h/J = 0.5$ comes from the disordered spins remaining in the low- T ordered state (see below). Below the transition temperature, the magnetization process shows plateaus at $\langle m \rangle = \pm 1/3$ as shown in Fig. 3(b), where $m = \sum_{\nu,i} S_{\nu,i}/N_s$. The plateau state shows a partially-disordered AF (PDAF) ordering, which consists of the stacking of AF-ordered square lattices and disordered spins sandwiched between AF layers, as shown schematically in the left inset of Fig. 4. This dimensionality reduction, i.e., 2D LRO in a 3D system, yields 2^L -fold degeneracy due to the twofold degeneracy of the AF ordering pattern in each layer, leading to $(3 \times 2^L - 3)$ -fold degeneracy in total. The factor 3 comes from the stacking directions x , y , and z , and -3 subtracts the double counting. The schematic picture in Fig. 4 shows one of these degenerate states. The magnetic ordering and degeneracy are confirmed by calculating the 2D AF order parameter in each xy , yz , and zx layer. We summarize the critical temperature T_c determined from these magnetic properties in the phase diagram in Fig. 3(c). T_c is finite at $0 < |h|/J < 8$, showing its maxima $T_c/J \sim 2$ at $h/J \sim \pm 4$. The transition is of first order, confirmed by a detailed analysis of the probability distribution of the internal energy (not shown).

A similar dimensionality reduction has also been found in the ground state of the fcc AF Ising model.¹²⁾ In addition, similar magnetization plateaus have also been found in both the fcc^{13),14)} and pyrochlore models.²⁾ In these systems, however, the plateau states appear above some finite critical value of the applied magnetic field. A peculiar feature of our inverse perovskite model is that the critical field is zero and the plateau phases for the positive and negative values of h touch with each other at $h = 0$ with the complete suppression of T_c , as shown in Fig. 3(c).

The macroscopic degeneracy in the case of $J = J_{\perp}$ and $h = 0$ is also lifted by introducing an anisotropy in the interaction, namely, $J \neq J_{\perp}$. First, let us consider the case of $J > J_{\perp}$. In the limit of $J_{\perp}/J \rightarrow 0$, the system is decomposed into independent 2D square lattices and disconnected sites. Therefore, the system undergoes the same phase transition as that in the 2D Ising model at $T_c/J = 2/\sinh^{-1} 1 \simeq 2.269$ ¹⁵⁾ and the ordered phase is the PDAF state in which the AF orderings occur independently in the xy square lattices. This xy -PDAF state is stabilized at low T in the entire region of $J > J_{\perp}$. The order parameter is the staggered magnetization of each xy plane; $m_{xy} = \sum_{\nu} (S_{\nu,1} - S_{\nu,2})/2L^2$, where the summation is taken over the spins within one xy layer. The transition is of second order, and the critical temperature T_c is determined by the Binder parameter¹⁶⁾ $g_{xy} = 1 - \langle m_{xy}^4 \rangle / 3 \langle m_{xy}^2 \rangle^2$. The results are plotted in the left half of Fig. 4. T_c decreases as J_{\perp}/J increases and goes continuously to zero when $J_{\perp}/J \rightarrow$

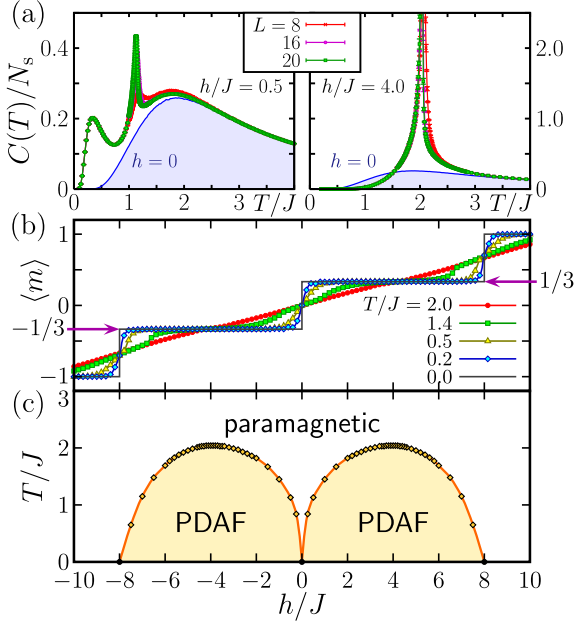


Fig. 3. (a) Temperature dependence of the specific heat at $h/J = 0.5$ (left) and 4.0 (right) for $J = J_\perp$. The data at $h = 0$ are shown for comparison. (b) Magnetization process at several temperatures. (c) Phase diagram at $J = J_\perp$. PDAF denotes the partially-disordered AF phase. The lines are guides for the eyes.

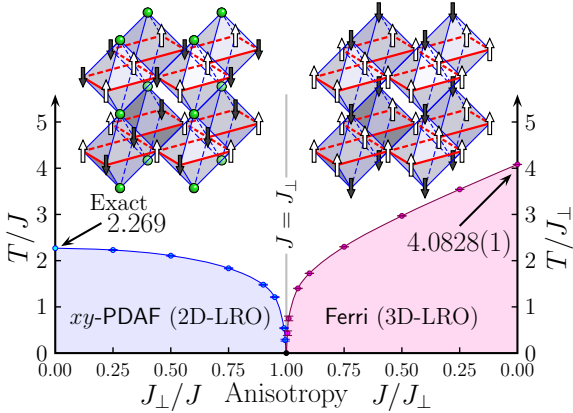


Fig. 4. Phase diagram for the anisotropy in the interaction (J, J_\perp) at $h = 0$. The lines are guides for the eyes. Schematic pictures of $xy\text{-PDAF}$ state (left) and 3D Ferri state (right) are also shown. Open (filled) arrows denote up (down) spins, and balls represent disordered spins.

1. We also examined the universality class of this $xy\text{-PDAF}$ transition by the finite-size scaling (FSS) analysis; $\langle m_{xy}^2 \rangle = L^{-2\beta/\nu} f(tL^{1/\nu})$, where f is a scaling function and $t = T/T_c - 1$ is the reduced temperature. We confirmed that the transition belongs to the 2D Ising universality with the exponents $\beta = 1/8$ and $\nu = 1$.¹⁷⁾

On the other hand, on the opposite side, i.e., $J < J_\perp$, we find a phase transition to the ferrimagnetic (Ferri) 3D-LRO state, as shown schematically in the right inset of Fig. 4. The order parameter is defined by $m_f = \sum_\nu (S_{\nu,1} + S_{\nu,2} - S_{\nu,3})/3L^3$. The Ferri ground state has twofold degeneracy, $m_f = \pm 1/3$ corresponding to the spin configurations $(S_{\nu,1}, S_{\nu,2}, S_{\nu,3}) = (1, 1, -1)$ and $(-1, -1, 1)$, respectively. In this case also, the transi-

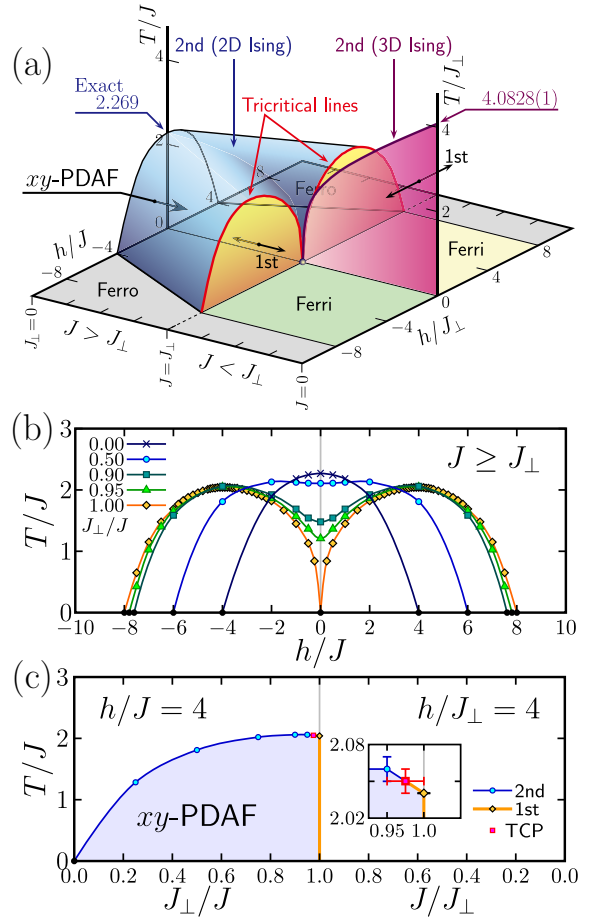


Fig. 5. (a) Phase diagram of the inverse perovskite AF Ising model in the T - h - (J, J_\perp) space. (b) h - T phase diagrams for several values of J_\perp/J for $J \geq J_\perp$. (c) (J, J_\perp) - T phase diagram at $h = 4 \max(J, J_\perp)$. The lines are guides for the eyes, and TCP denotes the tricritical point.

tion is of the second order, and the values of T_c obtained by the Binder analysis are plotted in the right half of Fig. 4. T_c decreases as J/J_\perp increases and goes continuously to zero when $J/J_\perp \rightarrow 1$, as in the case of $J > J_\perp$. We also confirmed that the transition belongs to the 3D Ising universality class by the FSS analysis. For instance, in the limit of $J/J_\perp \rightarrow 0$, we obtained $T_c/J_\perp = 4.0828(1)$ and the critical exponents $\beta = 0.32(1)$ and $\nu = 0.625(7)$, which are consistent with the 3D Ising exponents, $\beta = 0.325$ and $\nu = 0.63$,¹⁸⁾ within the statistical errors.

The effect of anisotropy J/J_\perp at $h = 0$ is summarized as follows: The anisotropy lifts the macroscopic degeneracy and induces the phase transition at finite T ; the $xy\text{-PDAF}$ state appears for $J > J_\perp$ and the 3D Ferri state for $J < J_\perp$. The two different ordered phases touch with each other at the isotropic point $J = J_\perp$. Here, T_c goes continuously to zero on both the sides. The universality class of the transition is different between the cases of $J > J_\perp$ and $J < J_\perp$; the 2D Ising one in the former due to the dimensionality reduction and the 3D Ising one in the latter. These properties are contrasted to those of the fcc system. In the isotropic fcc model, a first-order phase transition takes place at finite T , namely, there is no suppression of T_c .^{12), 19)} It was also proposed that the

critical exponents change continuously²⁰⁾ when a similar anisotropy in the interactions is introduced.

On the basis of the above analyses obtained from applying magnetic field h or from introducing the anisotropy $J \neq J_{\perp}$, the peculiarity of the isotropic model with $J = J_{\perp}$ and $h = 0$ is revealed: The model has a critical point at $T = 0$ in the sense that the transition temperatures are suppressed down continuously to zero in both the cases of $|h| \rightarrow 0$ and $J/J_{\perp} \rightarrow 1$.

To further clarify the behavior around the critical point, we investigate the model by changing both the h and J/J_{\perp} values. The phase diagram in a wide range of parameters is shown in Fig. 5(a). When we decrease J_{\perp}/J from 1, two PDAF phases in the case of $J = J_{\perp}$ in Fig. 3(c) gradually merge into one, as shown in Fig. 5(b). On the other hand, in the region of $J < J_{\perp}$, the magnetic field is a symmetry-breaking field of the Ferri ordering at $h = 0$, and therefore, the finite- T phase transition disappears at $h \neq 0$. Hence, at finite h , the PDAF ordered phase suddenly terminates at $J = J_{\perp}$. This behavior is studied in detail by changing J/J_{\perp} . For instance, Fig. 5(c) shows the result at $h = 4 \max(J, J_{\perp})$. Since the phase transition at the isotropic case $J = J_{\perp}$ is of the first order as discussed earlier and since no transition exists at finite T for $J < J_{\perp}$, we have a discontinuous phase boundary at $J = J_{\perp}$ below T_c . This discontinuous boundary slightly extends to $J > J_{\perp}$ and terminates at a tricritical point beyond which the transition becomes continuous, as shown in Fig. 5(c). The tricritical behavior appears for $0 < |h|/J < 8$, resulting in the tricritical lines which start from $(J_{\perp}/J, h/J, T/J) = (1, 0, 0)$ and end at $(1, \pm 8, 0)$, as shown in Fig. 5(a). Note that the tricritical lines are not in the $J = J_{\perp}$ plane, but in a very narrow region, $0.95 < J_{\perp}/J \leq 1$.

All the features above are shown in Fig. 5(a) with the ground-state phase diagram which is easily obtained by minimizing the energy of one octahedron. The figure includes the PDAF phase for $J > J_{\perp}$ (blue region), the discontinuous surface in the $h = 0$ plane for $J < J_{\perp}$ (purple plane), and the tricritical lines (red curves) surrounding the discontinuous phase boundaries at the edges of the PDAF state (orange surfaces). This global phase diagram clearly demonstrates the peculiarity of the critical point at $J = J_{\perp}$ and $h = 0$, where all the critical temperatures, for both first- and second-order transitions, are suppressed down continuously to zero.

The absence of LRO at the critical point is understood as follows. When we start from a PDAF ordered state, we can generate an anti-phase domain in the AF-ordered square lattice without any energy cost because of the partial disorder. This leads to the destruction of PDAF ordering and to the formation of a degenerate ground-state manifold. The situation is similar when we start from the Ferri 3D-LRO state. These anti-phase domains cost a finite energy when we introduce the magnetic field h and/or anisotropy J/J_{\perp} and hence finite- T phase transitions immediately emerge around the critical point.

In summary, by using the exchange Monte Carlo method, the phase diagram of the AF Ising model on the inverse perovskite lattice has been clarified in the parameter space of the uniform magnetic field and the

anisotropy in the interaction. It has revealed an unusual character of the $T = 0$ critical point, which drags the surrounding critical lines and surfaces at $T \neq 0$ toward absolute zero temperature. Neither fcc nor pyrochlore AF Ising model exhibits such a behavior.

In the fcc system at the isotropic point, there is no suppression of T_c and a first-order transition to the 2D-LRO state takes place.^{12),19)} In the isotropic pyrochlore system, although the ground state has macroscopic degeneracy as that in the present system, the degeneracy remains until a finite magnetic field is applied ($|h| < 2J$).²⁾

The pyrochlore system has attracted interest due to the degenerate ground state manifold, and the effects of the Heisenberg-type interaction and quantum fluctuations have been examined intensively in the search for an “order from disorder” phenomenon or a spin-liquid state. Since the degenerate ground state in the inverse perovskite model is at a more unusual critical state with competing orders, it would be more interesting and worthwhile to study such effects in the inverse perovskite system. In particular, quantum fluctuations may easily destroy the orderings barely stabilized around the $T = 0$ classical critical point, which may open possibilities for quantum spin-liquid phases or exotic quantum orders.

One of the authors (D.T.) thanks T. Misawa for useful discussions. This work was supported by Grants-in-Aid for Scientific Research on Priority Areas under the grant numbers 17071003, 16076212, 17740244, and 16GS0219 from the Ministry of Education, Culture, Sports, Science and Technology. A part of our computation has been done using the facilities of the Supercomputer Center, Institute for Solid State Physics, University of Tokyo.

- 1) For instance, *Frustrated Spin Systems*, ed. H. Diep (World Scientific, Singapore, 2005), and references therein.
- 2) For a review, R. Liebmann: *Statistical Mechanics of Periodic Frustrated Ising Systems* (Springer-Verlag, Berlin, Tokyo, 1986).
- 3) G. H. Wannier: Phys. Rev. **79** (1950) 357.
- 4) R. M. F. Houtappel: Physica **16** (1950) 425.
- 5) K. Husimi and I. Syozi: Prog. Theor. Phys. **5** (1950) 177.
- 6) P. W. Anderson: Phys. Rev. **102** (1956) 1008.
- 7) A. P. Ramirez *et al.*: Nature **399** (1999) 333.
- 8) T. He *et al.*: Nature **411** (2001) 54.
- 9) K. Takenaka and H. Takagi: Appl. Phys. Lett. **87** (2005) 261902.
- 10) K. Hukushima and K. Nemoto: J. Phys. Soc. Jpn. **65** (1996) 1604.
- 11) T. Yoshioka, A. Koga and N. Kawakami: J. Phys. Soc. Jpn. **73** (2004) 1805.
- 12) A. Danielian: Phys. Rev. Lett. **6** (1961) 670; A. Danielian: Phys. Rev. **133** (1964) A1344.
- 13) J. L. Lebowitz, M. K. Phani and D. F. Styer: J. Stat. Phys. **38** (1985) 413.
- 14) S. Kämmerer *et al.*: Phys. Rev. B **53** (1996) 2345.
- 15) L. Onsager: Phys. Rev. **65** (1944) 117.
- 16) D. P. Landau and K. Binder: *A Guide to Monte Carlo Simulations in Statistical Physics* (Cambridge University Press, Cambridge, 2000).
- 17) B. Kaufmann and L. Onsager: Phys. Rev. **76** (1944) 1244.
- 18) J. C. LeGuillou and J. Zinn-Justin: Phys. Rev. Lett. **39** (1977) 95.
- 19) M. K. Phani *et al.*: Phys. Rev. Lett. **42** (1979) 577.
- 20) S. Onoda, Y. Motome and N. Nagaosa: Phys. Rev. Lett. **92** (2004) 236403.